INVESTIGATIONS OF TURBULENT MIXING REGIONS

Thesis by

Arnold M. Kuethe

In Partial Fulfillment of the Requirements for the Degree of

Doctor of Philosophy

California Institute of Technology

Pasadena, California

1933

Summary.

The turbulent mixing of two jets of fluid of the same density is investigated theoretically by means of Prandtl's theory of turbulence and the results compared with experiment. The mixing length is assumed proportional to the breadth of the mixing region with a proportionality constant which is the only empirical constant in the theory.

In Part II a solution obtained by Tollmien for the mixing region of a plane jet, in which he considers the fluid bounding the jet at rest, is extended to the general case of the mixing of two streams of different velocities separated initially by a plane surface. Distributions of the tangential and normal velocities in the mixing region are given.

Part III deals with the turbulent mixing region surrounding an axially symmetric jet issuing into fluid at rest. The problem is solved, as far as the core of potential flow extends, by the application of a new method of approximation directly to the partial differential equation of motion. The velocity field, as determined by a second approximation to the velocity profiles, is given. An extension of the method of solution, applicable to problems in which the velocity profiles differ widely, is mentioned.

In Part IV the empirical constant occurring in the assumption for the mixing length is evaluated. Velocity profiles in the mixing region of an axially symmetric jet were measured by means of a pitot tube and good agreement is found between theory and experiment.

Finally, some measurements of the velocity fluctuations, made by means of the hot-wire anemometer, are given.

I. Introduction.

This investigation deals with some of the many cases of the turbulent mixing of two parallel streams of fluid of the same density moving at different velocities. The boundaries of the open jet wind tunnel and of the slipstream of a propeller are two very frequent cases to which the results apply.

Considering first a perfect fluid, it is well known that a surface of discontinuity in the velocity, though not in the pressure, may exist at the boundary separating the two streams. Helmholtz (1) first pointed out the possibility of the existence of this surface, but proved it to be unstable*, i.e., a slight disturbance will build up into a regular succession of vortices travelling along the surface. The vena contracta and the boundaries of the dead water region behind a flat plate are examples which have been treated by Kirchhoff, Rayleigh and others.

When a jet of viscous fluid issues at a low velocity into fluid at rest a regular succession of vortices is given off at the rim. As the velocity is increased beyond a certain low limit this periodic flow is replaced by a turbulent mixing region.

Turbulence, as distinct from those cases in which a regular succession of vortices is formed, is characterized by an irregular fluctuating motion superposed on a mean flow. These fluctuations give rise to a momentum transport

---

* On the other hand, Ackeret (Helvatica Physica Acta, I:V, p. 301, (1928)) has shown that, for hyper-sonic velocities, the surface is stable.

between neighboring fluid regions and, as a result, "apparent stresses" will act between these regions. If we consider a flow, the main component of which is in the x direction, its magnitude being a function mainly of y, the momentum transport will depend upon the velocity gradient and the most important apparent stress will be τ_{xy}. Prandtl (2) gives the expression

1.1) $$\tau_{xy} = \rho l^2 \left(\frac{du}{dy}\right)\left|\frac{du}{dy}\right|$$

where ρ is the density of the fluid, u is the mean velocity, and l the so-called "mixing length". l is analogous to the mean free path in the Kinetic Theory of Gases and is proportional to the mean distance which a fluid mass will travel in the y direction without losing its initial momentum. In cases of free turbulence, i.e., cases in which there are no confining walls, the very simple assumption that l is constant over any cross-section and proportional to the breadth of the mixing region gives results in good agreement with practice.

Tollmien (3), with the aid of (1.1), solved the problem of the plane jet issuing into a medium at rest and also obtained a solution valid at great distances from an axially symmetrical jet. These solutions hold for a wide range of velocities and this is not surprising when we consider the strong discontinuity in the velocity at the rim of the jet. Very large velocity disturbances result and the completely turbulent state is realized at a comparatively low velocity.

The object of the present work was to extend Tollmien's results to other cases of practical importance. We treat at first the two dimensional problem and later that of the axially symmetric jet.

II. The Plane Jet.

The arrangement, as shown in Figure 1, in which η_1 and η_2 are the boundaries of the turbulent mixing region, finds practical application both in the case of the open jet wind tunnel and the propeller slip-stream. The limit of its applicability due to the finite diameter of the wind tunnel or the propeller, will be discussed in Part III.

Tollmien's solution for $u_2 = 0$ is here extended to the case in which u_2 has any value from 0 to u_1. Since the flow in the mixing region will have its main component parallel to x, we can assume that no appreciable pressure difference exists normal to x between the two streams, and, since the pressure in the jets outside the mixing region is constant, the pressure gradients can be completely neglected. Hence for flow in the x direction we need only consider the first equation of motion, and this reduces to

$$u \frac{\partial u}{\partial x} + v \frac{\partial u}{\partial y} = \frac{\partial \tau_{xy}}{\partial y} \tag{2.1}$$

where v is the y component of the mean velocity and τ_{xy} is given by (1.1). This equation, combined with the continuity equation

$$\frac{\partial u}{\partial x} + \frac{\partial v}{\partial y} = 0 \tag{2.2}$$

and suitable boundary conditions then describes the field of flow in the mixing region.

Since an x gradient in u exists, from continuity, it follows that there is a v component. The value of this component at the low-velocity boundary of the mixing region we term the "suction velocity".

We assume

$$u = f(y/x)$$

i.e., that the breadth of the mixing region is proportional to x.

Hence the assumption that the mixing length is proportional to the breadth of the mixing region can be expressed as

2.3) $$l = cx$$

where c is an empirical constant.

We obtain, from (2.3), the stream function

$$\psi = xF\left(\frac{y}{x}\right)$$

and, consequently,

2.4) $$\begin{cases} u = F' \\ v = -F + \frac{y}{x}F' \end{cases}$$

Substituting (1.1), (2.3) and (2.4) in (2.1) leads to the ordinary differential equation

2.5) $$F(\eta) + F'''(\eta) = 0$$

where

$$\eta = \frac{y}{x\sqrt[3]{2c^2}}$$

The solution to (2.5) can be expressed in the following form

2.6) $$F(\bar{\eta}) = d_1 e^{-\bar{\eta}} + d_2 e^{\bar{\eta}/2}\cos\frac{\sqrt{3}}{2}\bar{\eta} + d_3 e^{\bar{\eta}/2}\sin\frac{\sqrt{3}}{2}\bar{\eta},$$

where $\bar{\eta} = \eta - \eta_1$, and d_1, d_2, and d_3 are constants. To determine these constants and the boundaries of the mixing region we choose the boundary conditions,

2.7) $$\text{at } \eta = \eta_1 ; \bar{\eta} = 0 \begin{cases} u = u_1 \\ \frac{\partial u}{\partial y} = \frac{\partial u}{\partial \bar{\eta}} = 0 \\ v = 0 \end{cases} ; \text{ at } \eta = \eta_2 ; \bar{\eta} = \bar{\eta}_2 \begin{cases} u = u_2 \\ \frac{\partial u}{\partial y} = \frac{\partial u}{\partial \bar{\eta}} = 0 \end{cases}$$

The condition v=0 at the high velocity boundary is an assumption the validity of which may depend upon the details of the experimental arrangement outside the neighborhood of the mixing region. Experiments indicate, however, that the assumption is justified in a large number of cases of practical importance.

In terms of the function $F(\bar{\eta})$, (2.7) reduces to

2.8) $$\begin{cases} F(0) = \eta_1 u_1 & F'(\bar{\eta}_2) = u_2 \\ F'(0) = u_1 & \\ F''(0) = 0 & F''(\bar{\eta}_2) = 0 \end{cases}$$

From the first three conditions we get simply,

2.9) $$\begin{cases} d_1 = \frac{u_1}{3}(\eta_1 - 1) & \\ d_2 = \frac{u_1}{3}(1 - 2\eta_1) & d_3 = 0.577\, u_1 \end{cases}$$

These expressions are substituted in (2.6) and $F''(\bar{\eta}_2) = 0$ yields

2.10) $$\eta_1 = \frac{e^{-1.5\bar{\eta}_2} - \cos\frac{\sqrt{3}}{2}\bar{\eta}_2 + \sqrt{3}\sin\frac{\sqrt{3}}{2}\bar{\eta}_2}{e^{-1.5\bar{\eta}_2} - \cos\frac{\sqrt{3}}{2}\bar{\eta}_2 - \sqrt{3}\sin\frac{\sqrt{3}}{2}\bar{\eta}_2}$$

$F'(\bar{\eta}_2) = u_2$ gives

2.11) $$m = \frac{u_2}{u_1} = e^{\bar{\eta}_2/2}\left[\cos\frac{\sqrt{3}}{2}\bar{\eta}_2 - \frac{2}{\sqrt{3}}\left(\eta_1 + \frac{1}{2}\right)\sin\frac{\sqrt{3}}{2}\bar{\eta}_2\right]$$

Substituting (2.10) for η_1 in (2.11) we get m as a function of $\bar{\eta}_2$. This function is plotted and for a given value of m the corresponding value of $\bar{\eta}_2$ is substituted in (2.10), giving η_1. η_2 is then obtained from the formula $\bar{\eta}_2 = \eta_2 - \eta_1$. The results are shown in Figure 2.

It is seen that for m=0 the mixing region is not symmetrical about the extension of the boundary initially separating the two jets, but, as m increases, the boundaries gradually approach a position symmetrical about this line. Figure 3, in which u velocity profiles for three values of m are plotted, shows clearly this transition. If $\bar{\eta}_2$ is replaced by $2\eta_2$ or $-2\eta_1$ and the series expansions for the various terms are substituted in (2.11), we find, near m=1,

2.12) $$\eta_1 = -\eta_2 = \sqrt[3]{\frac{3}{2}(1-m)}$$

where terms of order η_1^5 are neglected.

To find the velocity profile, given any m (≥ 0) (if the given value

is greater than unity, its reciprocal is to be used), the corresponding value for η_1 , as read from Figure 2, is substituted in (2.9), giving the values for the d's. $F(\overline{\eta})$ is then obtained from (2.6) and the corresponding velocity profiles from (2.4), where it must be remembered that the scale of y/x has been reduced by the factor $\sqrt[3]{2c^2}$.

To show the change in shape resulting from a change in m the velocity profiles of Figure 3 are re-plotted in Figure 4 where ordinates and abscissae are chosen so that all profiles have the same limits. Figure 5 shows the corresponding distributions for the normal velocities. In some cases it is of interest to know the suction velocities as a function of m. This is shown in Figure 6.

Measurements of the mean velocities in the mixing region at the boundary of the open jet wind tunnel in Göttingen show that $c = 0.0174$. Hence, $\sqrt[3]{2c^2} = 0.0845$ gives good agreement between theory and experiment.

Tollmien carried out an investigation of the pressure difference existing between the center of the mixing region and the undisturbed flow by substituting his results for u, v, τ ($u_2 = 0$) in the second equation of motion

$$u\frac{\partial v}{\partial x} + v\frac{\partial v}{\partial y} = -\frac{1}{\rho}\frac{\partial p}{\partial y} + \frac{1}{\rho}\frac{\partial \tau}{\partial x}$$

and determining p by integrating with respect to y. He found this difference in pressure to be $0.00482\,\frac{\rho}{2}u_1^2$, which, if taken into account, would not appreciably alter the stream lines. Hence we can safely say that neglecting this quantity for the cases considered above is justifiable.

III. The Axially Symmetric Jet.

The case of the discharge of an axially symmetric jet into fluid at rest occurs very frequently, especially in experimental arrangements. Tollmien's solution for this case in which he considers the jet as issuing from a point holds very well for values of x greater than about eight diameters. However, if we wish to obtain a solution valid near the mouth of the jet, it appears impossible to transform the equation for the mean motion into a total differential equation. Accordingly, a method for obtaining an approximate solution was applied directly to the partial differential equation.

We can form a qualitative picture of the flow from a consideration of the building up of the turbulent mixing region. This region, originating at the rim of the jet mouth will form an annular ring enclosing a core of potential flow in which the velocity is constant and equal to the outflow velocity. At a point $x = x_1$ this core will vanish and the entire jet then becomes a turbulent mixing region. A cross-section of the flow is shown in Figure 7. Region A consists of the annular mixing region surrounding the core of potential flow. In region B the entire jet is a mixing region and the central velocity u_o decreases as x increases. The velocity profiles and the x gradient of u_o finally reach an asymptotic state as the fluid enters region C. In C the central velocity is inversely proportional to the distance from some point near the jet mouth and all profiles are similar, i.e., plotting u/u_o against y/b where y is the radial distance of a point from the axis and b is the breadth of the jet, all points fall on a single curve. It is in this last region that Tollmien's solution is valid.

At the point $x = x_1$, i.e., where the potential core vanishes, we can, for physical and mathematical reasons, expect considerable difficulty in finding a solution reasonably close to practice. Consequently we will consider at first only region A.

For the same reasons as in Part II the pressure gradients are neglected and the equation for the mean motion is

3.1) $$u\frac{\partial u}{\partial x} + v\frac{\partial u}{\partial y} = \frac{1}{\rho y}\frac{\partial}{\partial y}(\tau y)$$

The continuity equation is

3.2) $$\frac{\partial}{\partial x}(uy) + \frac{\partial}{\partial y}(vy) = 0$$

For region A we have the following boundary conditions:

3.3) $$\text{at } y = d \begin{cases} u = 1 \\ \frac{\partial u}{\partial y} = 0 \\ v = 0 \end{cases} \quad ; \quad \text{at } y = d + b \begin{cases} u = 0 \\ \frac{\partial u}{\partial y} = 0 \end{cases}$$

where d is the radius of the potential core and $v = 0$ is an assumption, justified, as for the plane jet, by experimental results.

At $x = 0$, $y = 1$, (taking the jet mouth to be of unit radius) equation (3.1) reduces to the two dimensional equation (2.1), so that, the limiting profile is that for $m = 0$ in Figure 4. Then, as x increases, there must be a gradual transition from this profile to that obtained by Tollmien for x large. These two solutions are shown in Figure 8.

In both cases the mixing length l was taken proportional to the breadth of the mixing region but this is justified only when the profiles are similar. However, since the profiles do not differ markedly, we can, to a good approximation, again set

3.4) $$l = cb$$

where the value of c is not the same as it was in Part II. Substituting the expressions (1.1) and (3.4) in (3.1) we obtain

$$3.5) \qquad u\frac{\partial u}{\partial x} + v\frac{\partial u}{\partial y} = \frac{c^2 b^2}{y}\frac{\partial}{\partial y}\left\{\left(\frac{\partial u}{\partial y}\right)\left|\frac{\partial u}{\partial y}\right|y\right\}$$

To solve this differential equation approximately we first assume, as a first approximation, a reasonable velocity distribution in the mixing region. Then, by means of the differential equation we obtain a second approximation to the solution.

We can consider u as a function of y, d, and b, where d and b are, as yet, undetermined. We assume, for simplicity, that u_1, where here as in subsequent expressions the subscript refers to the order of the approximation, is a function only of θ, defined by the formula

$$3.6) \qquad u_1 = f(\theta) \quad \text{where} \quad \theta = \frac{y-d}{b}$$

This assumption expresses the fact that the first approximation is made up of similar profiles. The dependence expressed by (3.6) is in complete agreement with the results of Part II at the rim of the jet mouth when the origin of coordinates is transformed to that point.

The simple expression

$$3.7)^* \qquad u_1 = \left(1-\theta^{3/2}\right)^2$$

satisfies the boundary conditions (3.3) and, as is shown in Figure 8,

---

* The corresponding expression

$$u = \left\{1-\left(y/b\right)^{3/2}\right\}^2$$

was found by Miss Swain (4) and Schlichting (5) as a first approximation to the velocity profiles for the axially symmetric and the plane windshadows respectively.

is reasonably close to the limiting profile at x=0. It was therefore chosen as a first approximation to the profiles in region A. The corresponding value of v_1, as determined from (3.2) is

3.8) $$v_1 = -\frac{1}{y}\int_d^y \frac{\partial u_1}{\partial x} y\, dy$$

In the first approximation (3.7) the quantities d and b are still unknown. The first attempt to find these parameters was made by means of the well known "Momentum Theorem". Multiplying both sides of (3.5) by y and integrating with respect to y, we get

3.9) $$uv_y - \frac{\partial}{\partial x}\int_y^{d+b} u^2 y\, dy = c^2 b^2 \left(\frac{\partial u}{\partial y}\right)^2 y$$

This relation is specialized for y= 0, corresponding to the axis of the jet. Then

3.10) $$\int_0^{d+b} u^2 y\, dy = \text{const} = \int_0^1 y\, dy = 0.5$$

where the integral represents, to a factor of 2π, the total momentum passing any section per second. This is set equal to the momentum issuing at the mouth of the jet. Secondly we place y in (3.9) equal to unity, corresponding to the point in the mixing region on the cylindrical extension of the jet mouth. We now substitute $u = u_1$ and $v = v_1$ from (3.7) and (3.8) in (3.10). There result two relations between b, d, $\frac{db}{dx}$ and $\frac{dd}{dx}$ from which we can easily determine b and d as functions of x. This method of building up a first approximation is similar to one suggested by Prof. von Kármán and applied by Pohlhausen (6) in the theory of the laminar boundary layer.

To obtain a second approximation u_2, we substitute the first approximation u_1, v_1 in the left side of (3.9) and identify the right side with the second approximation. One integration then gives

3.11) $$u_2 = \int_y^{d+b} \sqrt{\frac{1}{c^2 b^2 y}\left\{u_1 v_1 y - \frac{\partial}{\partial x}\int_y^{d+b} u_1^2 y\, dy\right\}}\; dy$$

This expression is so constructed that the boundary conditions $u_2 = \frac{\partial u_2}{\partial y} = 0$ at y=d+b are satisfied. Unfortunately, the second approximation had a strong deviation, amounting to from five to ten percent, from u_1 at the inner boundary y=d of the mixing region of the first approximation. This behavior would have been very difficult to correct since it signifies an overlapping of the mixing regions for the two approximations. Accordingly a method, suggested by Dr. Tollmien, by which the coincidence of the boundaries of the two approximations was immediately insured, was applied.

We shall delay for the moment the determination of the parameters b and d in the first approximation in order to develop a different and more convenient method for proceeding from u_1 to u_2. For this purpose we write the equation of motion (3.5) in the form

3.12) $$2b^2c^2\frac{\partial^2 u}{\partial y^2} = -\frac{u\frac{\partial u}{\partial x}}{\frac{\partial u}{\partial y}} - v - \frac{b^2c^2}{y}\frac{\partial u}{\partial y}$$

The denominator $\frac{\partial u}{\partial y}$ causes no singularity at its vanishing points, since, at these points $\frac{\partial u}{\partial x}$ vanishes with at least the same order. We now place u_1 in the right and u_2 in the left side of (3.12) and get, for the second approximation,

3.13) $$\frac{\partial u_2}{\partial y} = \int_d^y \frac{1}{2b^2c^2}\left\{-\frac{u_1\frac{\partial u_1}{\partial x}}{\frac{\partial u_1}{\partial y}} - v_1 - \frac{b^2c^2}{y}\frac{\partial u}{\partial y}\right\} dy$$

3.14) $$u_2 = \int_y^{d+b} \int_d^y \frac{1}{2b^2c^2} \left[- \frac{u_1 \frac{\partial u_1}{\partial x}}{\frac{\partial u_1}{\partial y}} - v_1 - \frac{b^2c^2}{y} \frac{\partial u_1}{\partial y} \right] dy\, dy$$

where the integration limits are chosen so that $\frac{\partial u_2}{\partial y} = 0$ at y=d, $u_2 = 0$ at y=d+b. According to the idea outlined above the boundaries of both approximations shall coincide, i.e., the boundary conditions $u_1 = u_2 = 1$ at y=d and $\frac{\partial u_1}{\partial y} = \frac{\partial u_2}{\partial y} = 0$ at y=d+b shall be satisfied. Then, from 3.13) and (3.14),

$$\int_d^{b+d} \frac{1}{2b^2c^2} \left[- \frac{u_1 \frac{\partial u_1}{\partial x}}{\frac{\partial u_1}{\partial y}} - v_1 - \frac{b^2c^2}{y} \frac{\partial u_1}{\partial y} \right] dy = 0$$

$$\int_d^{b+d} \int_d^y \frac{1}{2b^2c^2} \left[- \frac{u_1 \frac{\partial u_1}{\partial x}}{\frac{\partial u_1}{\partial y}} - v_1 - \frac{b^2c^2}{y} \frac{\partial u_1}{\partial y} \right] dy\, dy = 1$$

We again assume that

$$u_1 = f(\theta)$$

Then the above conditions are transformed into

3.15) $$\frac{1}{2} \int_0^1 \left\{ u_1 (d' + b' \theta) - \frac{v_1}{c^2} - \frac{\partial u_1}{\partial \theta} \frac{1}{\theta + \delta} \right\} d\theta = 0$$

3.16) $$\frac{1}{2} \int_0^1 \int_0^\theta \left\{ u_1 (d' + b' \theta) - \frac{v_1}{c^2} - \frac{\partial u_1}{\partial \theta} \frac{1}{\theta + \delta} \right\} d\theta\, d\theta = 1$$

where $\delta = \frac{d}{b}$; $d' = \frac{1}{c^2} \frac{dd}{dx}$; $b' = \frac{1}{c^2} \frac{db}{dx}$

The expressions (3.7) and (3.8) are again used as a first approximation. If these are substituted in (3.15) and(3.16) the integrations can be carried out analytically and result in equations of the type

3.17) $$\begin{cases} b' f_1(\delta) + d' f_2(\delta) + f_3(\delta) = 0 \\ b' f_4(\delta) + d' f_5(\delta) + f_6(\delta) = 0 \end{cases}$$

Eliminating b' and d' successively gives

3.18) $$\begin{cases} b' = g_1(\delta) \\ d' = g_2(\delta) \end{cases}$$

or $$\frac{dd}{db} = \frac{g_2(\delta)}{g_1(\delta)} = b\frac{d\delta}{db} + \delta$$

Integration of this differential equation gives

$$\log \frac{b}{b_1} = \int_0^\delta \frac{g_1\, d\delta}{g_2 - g_1\delta}$$

where b_1 is an integration constant. The indicated integration can be carried out graphically and we have

3.19) $$\frac{b}{b_1} = f(\delta)$$

In order to determine b as a function of x we first plot the first equation of (3.18) and (3.19) and eliminate δ. Then, plotting $c^2\frac{d\chi}{db} = \frac{1}{b'}$ against b/b_1 and integrating, we obtain

3.20) $$\int_0^{\frac{b}{b_1}} \frac{d\left(\frac{b}{b_1}\right)}{b'} = \frac{c^2\chi}{b_1} = F\left(\frac{b}{b_1}\right)$$

where the condition that b=0 at χ=0 has been used. Further, from (3.19) we get δ as a function of $\frac{c^2\chi}{b_1}$. Then, from the relation d=δb,

3.21) $$\frac{c^2\chi}{b_1} = G\left(\frac{d}{b_1}\right)$$

Finally, by the condition d=1 at x=0, the integration constant b_1 is determined and we have both parameters in the form

3.22) $$\begin{cases} b = b(c^2\chi) \\ d = d(c^2\chi) \end{cases}$$

The boundaries of the mixing region are now fixed and u_2 is calculated from (3.14). Figure 9 shows two profiles, (δ = 0.04 and $\delta=\infty$) calculated in this manner. We know the limiting profile for $\delta=\infty$ to be that for the plane jet for m=0, where m is again the ratio of the

outside velocity to the jet velocity. This profile is also plotted in the figure and we see that the agreement between the second approximation and the exact solution is very good indeed.

Figure 9 shows the boundaries of the mixing region as given by (3.26) and also the lines of constant velocity as derived from the profiles for various values of δ. At $\delta=0$ the main correction term in u_1 vanished, having an infinite derivative at that point. The calculated profile was obviously considerably in error and consequently is not given here.

Since the momentum integral (3.10) has not yet been used in this process, we can, by means of it, determine how far we may consider the approximation good. The momentum for the profile at $\delta=0$ was twelve percent high while that for $\delta=0.04$ was still within two percent of the correct value. Hence the results are given only as far as or $c^2x = 0.044$.

Figure 9 shows that the lines of equal velocity are very nearly straight and we know that, for x small, they agree with those for the plane case. Furthermore Figure 8 shows that the divergence between profiles in region A is not large.

We can then easily predict the approximate flow picture if the jet is issuing into a moving fluid, which is the problem analogous to that considered in Part II for the plane jet. We know that the limiting conditions at the jet mouth will be those already considered for the plane jet. For m=0 the results of the foregoing analysis show that the change, both in the boundaries of the mixing region and the velocity profiles, is not large. This indicates that, for any m, the results of Part II for the plane jet can be used to a first approximation as far as the core of potential flow extends.

A refinement of the above method was applied in region B. However, near the point where the core of potential flow vanishes, the results were not in accord with experiment. Since, at this point, the physical behavior is not clear, making the assumption for δ very doubtful, no further attempt was made to describe the field of flow in this region.

The refined method consisted essentially of introducing non-similar profiles for the first approximation. Hence, u_1 must contain a "shape factor". For region A this proposal would lead, f.i., to an assumption

$$u_1 = \left[1 - \left(\frac{y-d}{b}\right)^p\right]^3$$

In addition to b and d we must now determine p, the shape factor, as a function of x. To carry out this determination we must have three conditions, one more than was required by the foregoing method. The momentum theorem (3.10) applied to u_1 gives us this third condition. This is differentiated with respect to x and we have three simultaneous differential equations to solve for b, d and p. The method of solution is similar to that outlined for the preceding method.

The utility of the above methods are, by no means, restricted to the above problem. They would be equally useful for the solution of various problems in laminar as well as turbulent flow. It is necessary, of course, to know the approximate shape of the velocity profiles. Higher approximations can be found by repeating the processes, though a considerable amount of calculation is involved.

Tollmien, by the method described in part II, carried out an investigation of the pressure difference between the center of the mixing

region and the undisturbed fluid for x large. This difference was found to be $-0.00295 \frac{\rho}{2} u_o^2$ where u_o is the central velocity in the jet at the point considered. This quantity is again negligible insofar as its consideration would alter the mean stream lines. Since the case considered above is intermediate between those considered by Tollmien no investigation of the pressure difference was made.

IV. Experimental.

For the purpose of evaluating the empirical constant in the calculation of Part III measurements were made of mean velocity distributions in an axially symmetric jet. Measurements of the velocity fluctuations as measured by the hot-wire anemometer are also given.

The arrangement, a longitudinal section of which is shown in Figure 11, was essentially an Eiffel type wind tunnel, the observation room being 140x188x188 centimeters and the outlet tube 76 centimeters in diameter. This part of the apparatus along with the motor and fan already existed so it was necessary to use an entrance small enough to permit an exploration of the velocity field as far as the asymptotic region.

A ten centimeter nozzle with fairing as shown in the figure was chosen. Air was drawn thru the arrangement by a two-bladed fan driven by a 7.5 horsepower A.C. motor, the speed of which was varied by varying the frequency of the current. With the outlet unobstructed, strong pulsations, backflow and rotation of the stream were observed. The bell mouth B eliminated the pulsations and the cone C, supported by three symmetrically placed guide-vanes, and the annular ring D eliminated the greater part of the backflow and rotation. In order to obtain a uniform velocity distribution across the inlet it was necessary that the nozzle have a cylindrical section at least 0.3 diameters in length.

A two-way traversing mechanism, loaned for the purpose by the Astrophysics Department, carried the measuring device. By bolting the device in positions I, II, and III successively it was possible

to obtain a longitudinal traverse of 9.3 diameters, which, along with a lateral motion of 27 centimeters was sufficient for the investigation.

Lateral traverses were made with a pitot tube at distances from 3 to 9.3 diameters from the jet mouth. Because of the high velocity gradient and large fluctuations about the mean velocity, measurements at distances less than three diameters could not be relied upon. However, Tollmien checked his results for the plane jet by comparison with measurements (7) made in Göttingen at the boundary of the jet, one half diameter from the mouth, of an open jet wind tunnel 2.24 meters in diameter. At that distance the mixing region was wide enough so that the above difficulty was not encountered. These measurements showed very good agreement between theory and experiment, so that, for the present purpose, the velocity field for distances between 0.5 and 3.0 diameters from the mouth could be interpolated very closely. The lines of equal velocity are shown in Figure 12, in which, for convenience in carrying over the theoretical results, the radial distance is measured in radii while the longitudinal is measured in diameters.

The dotted lines in the figure show the agreement between the theory of Part III and experiment for

$$c^2 = 0.00496$$

$$\text{i.e.,} \quad c = 0.0705$$

Figure 13 shows profiles at 0, 2, 4, 6, 8, and 9 diameters. The ordinates in this figure are displaced 0.2 along the velocity axis for each diameter from the mouth.

Figure 14 shows the scatter of the experimental points and their

agreement with the theoretical curve at x=4.5 diameters, which is the last point for which the theory is given. Aside from a small systematic difference near the center of the jet the agreement is quite good. This difference is in the direction indicated by the fact that the momentum calculated from the theoretical profile was two percent low. In Figure 15 the experimental points at x = 9.3 dia. are plotted along with Tollmien's solution for x large. There is again a very small systematic difference near the center.

The apparatus for measuring velocity fluctuations was developed by F. L. Wattendorf and the author and follows closely in principle that of earlier work by H. L. Dryden and the author at the Bureau of Standards (8). A detailed account of the arrangement will be given elsewhere. It consists essentially of an electrically heated platinum wire 0.0145 mm in diameter and about 3 mm long and a vacuum tube amplifier. The fluctuations in the resistance of the hot-wire, caused by fluctuations in the wind speed are impressed across the input of a five stage amplifier. The lag in amplitude of the resistance fluctuations is compensated for in the manner described in reference 8.

That the vertical hot-wire responds, to a first approximation, only to the fluctuation component in the direction of the mean flow can be appreciated from the following analysis. Due to the fact that one component of the fluctuations will be in the vertical direction its effect on the resistance of the hot-wire will be considerably less than that of the other two components. Neglecting the lag of the wire, which can have no effect here, the instantaneous resistance of the wire represents

$$q = \sqrt{(\bar{u}+u')^2 + v'^2 + w'^2}$$

where the dash indicates the mean value of the quantity over the time, u', v', w' are the three perpendicular components of the fluctuation velocity superposed on the mean flow and b is a small factor indicating the fact that the effect of w' is small. The hot-wire is included in a Wheatstone bridge arrangement, so that, the quantity passed on to the amplifier represents

$$a = q - \bar{q}$$

From the reading at the output of the amplifier we calculate $\sqrt{\overline{a^2}}$, and

$$\overline{a^2} = \overline{q^2} + \bar{q}^2 - 2\overline{q}\bar{q} = -\bar{q}^2 + \overline{q^2}$$

4.1) $$\overline{a^2} = \overline{u'^2} + \overline{v'^2} + b\overline{w'^2} + \bar{u}^2 - \bar{q}^2$$

since $\overline{q}\bar{q} = \bar{q}^2$ and $\overline{u'} = \overline{v'} = \overline{w'} = 0$.

If we assume that u', v', w' are small in comparison with $\bar{u}$, we can, to a good approximation, suppress all terms of degree higher than the second in the fluctuations. Then

$$\overline{q^2} \simeq \bar{u}^2 + \overline{v'^2} + b\overline{w'^2}$$

and, substituting this in (4.1), we obtain

4.2) $$\sqrt{\overline{a^2}} \simeq \sqrt{\overline{u'^2}}$$

Figure 16 shows the root mean square values of the velocity fluctuations in the core of potential flow. This curve represents three experiments with different hot-wires and each one shows a hump in the curve at x=3 diameters. Without a more intensive investigation no reason can be given for this effect. This figure also gives lateral traverses across the potential core at x=1.5 and x=2.5 diameters. These fluctuations, though rather high in

amplitude, apparently neither contribute to a shearing stress nor cause the potential core to vanish prematurely.

One lateral traverse was made in the asymptotic region at $x=9.0$ diameters, the results of which are plotted in Figure 17. The faired curve represents qualitatively the fluctuation field in this region.

The author wishes to express his appreciation to Dr. W. Tollmien and Dr. Th. von Kármán. The investigation was undertaken at the suggestion of Dr. Tollmien, who, along with Dr. von Kármán, made many helpful suggestions in the course of the work.

References

1) Lamb, H.: Hydrodynamics. Article 232

2) Prandtl, L.: Bericht über Untersuchungen zur ausgebildeten Turbulenz. Zeit. f. angew. Math. u. Mech. Bd. 5, p 136, (1925).

3) Tollmien, W.: Berechnung Turbulenter Ausbreitungsvorgänge. Zeit. f. angew. Math. u. Mech. Bd. 6, pp 468-478, (1926).

4) Swain, L. M.: Turbulent wake behind a body of revolution. Proc. Roy. Soc. Lond. 105A, pp 647-659, (1929).

5) Schlichting, H.: Über das ebene Windschattenproblem. Ingenieur Archiv I, p 533, (1930).

6) Pohlhausen, K.: Zür Integration der Differentialgleichung der laminaren Grenzschicht. Zeit. f. angew. Math. u. Mech. Bd. I, pp 252-268, (1921)

7) Göttingen Ergebnisse, II Lief., pp 69-73, (1923)

8) Dryden, H. L. and Kuethe, A. M.: The measurement of fluctuations of air speed by the hot-wire anemometer. N. A. C. A. Technical Report No. 320,(1929)

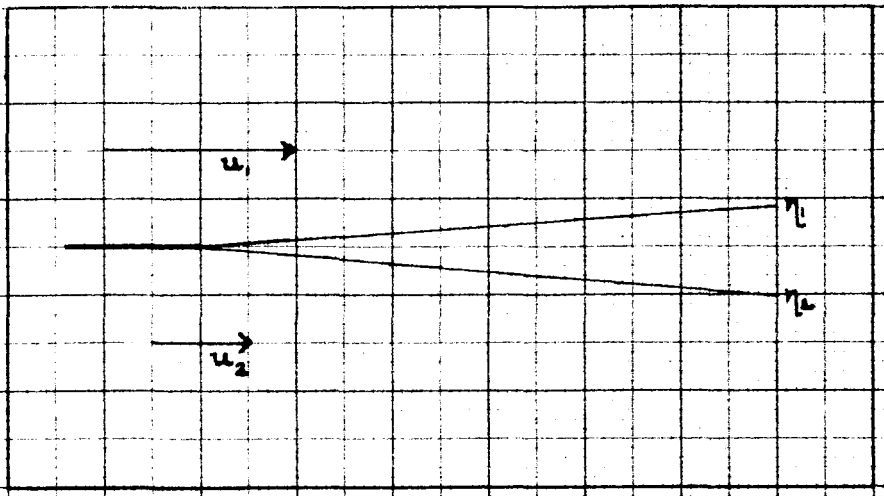

Figure 1. Schematic diagram of the Plane Jet

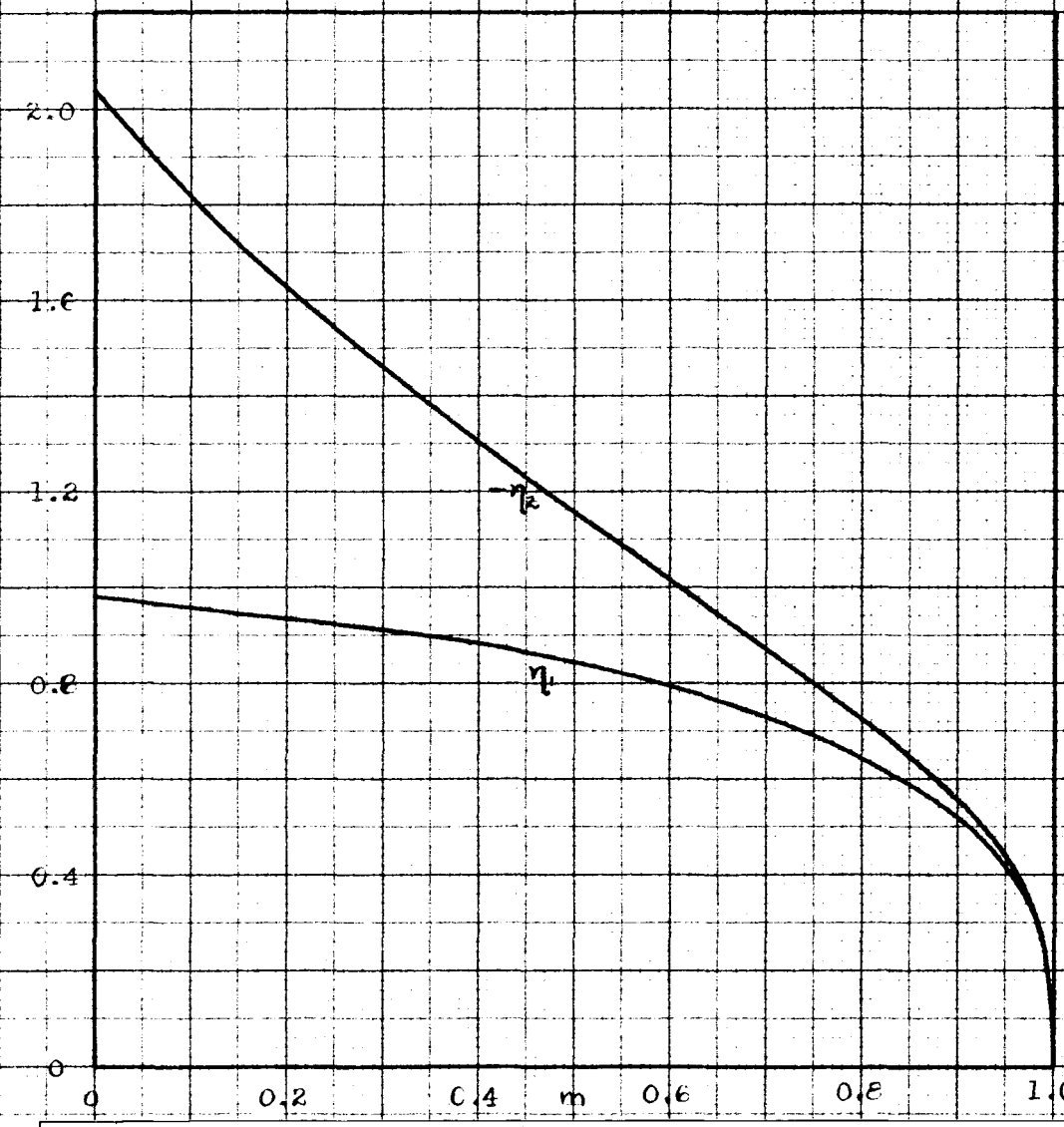

Figure 2. Boundaries of the Turbulent Mixing Region as Functions of $m = u_2/u_1$

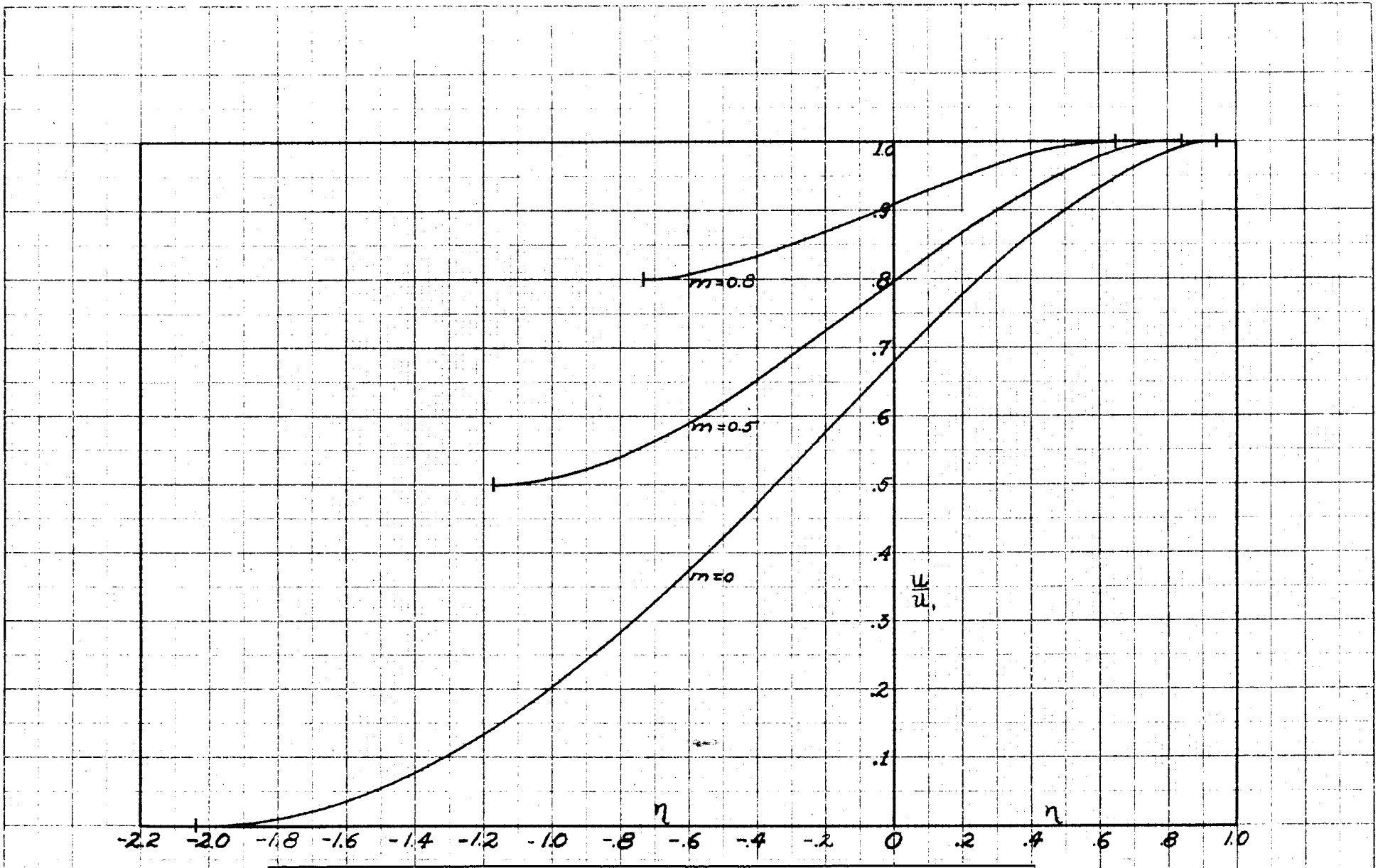

Figure 3. Distribution of u/u_1 for three values of $m = u_2/u_1$.

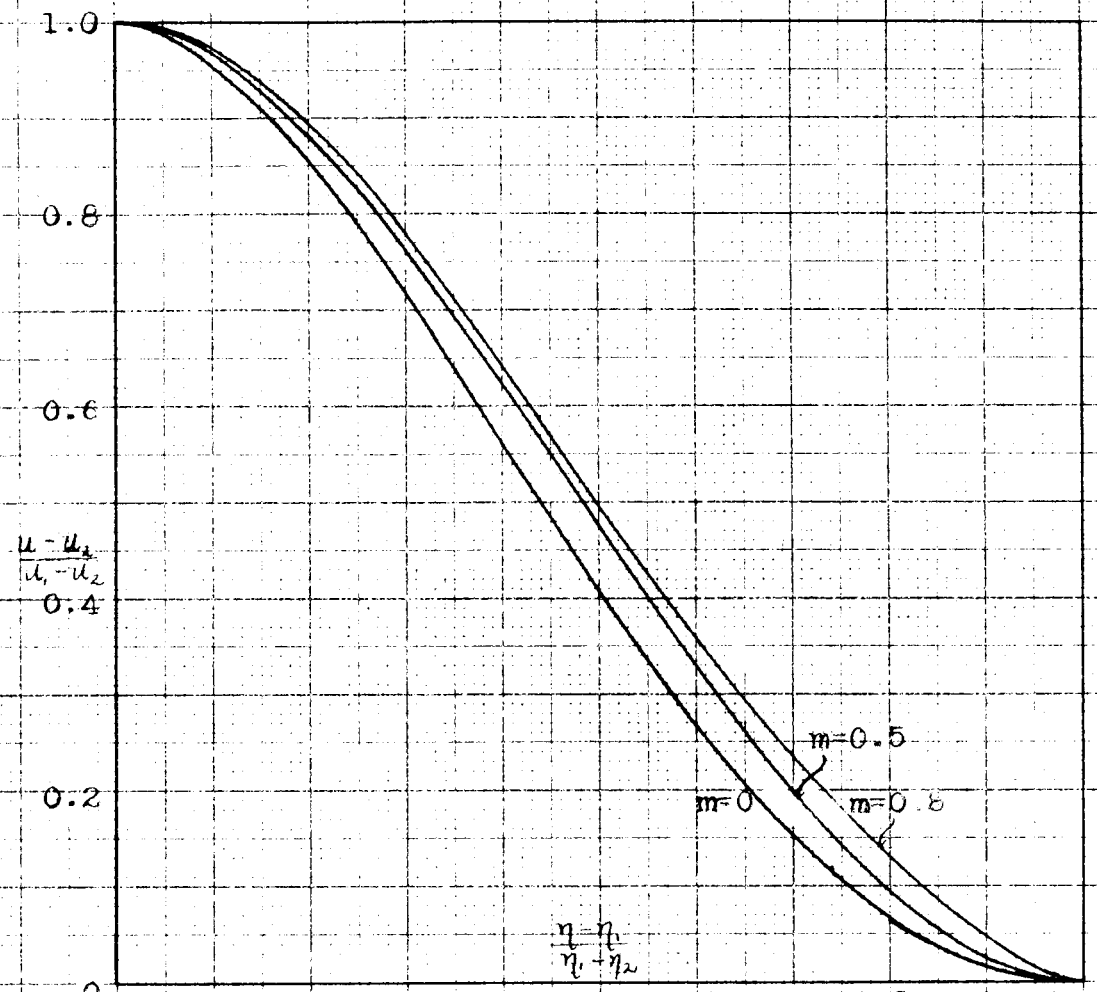

Figure 4. Distribution of $\frac{u-u_1}{u_1-u_2}$ for three values of $m = u_2/u_1$.

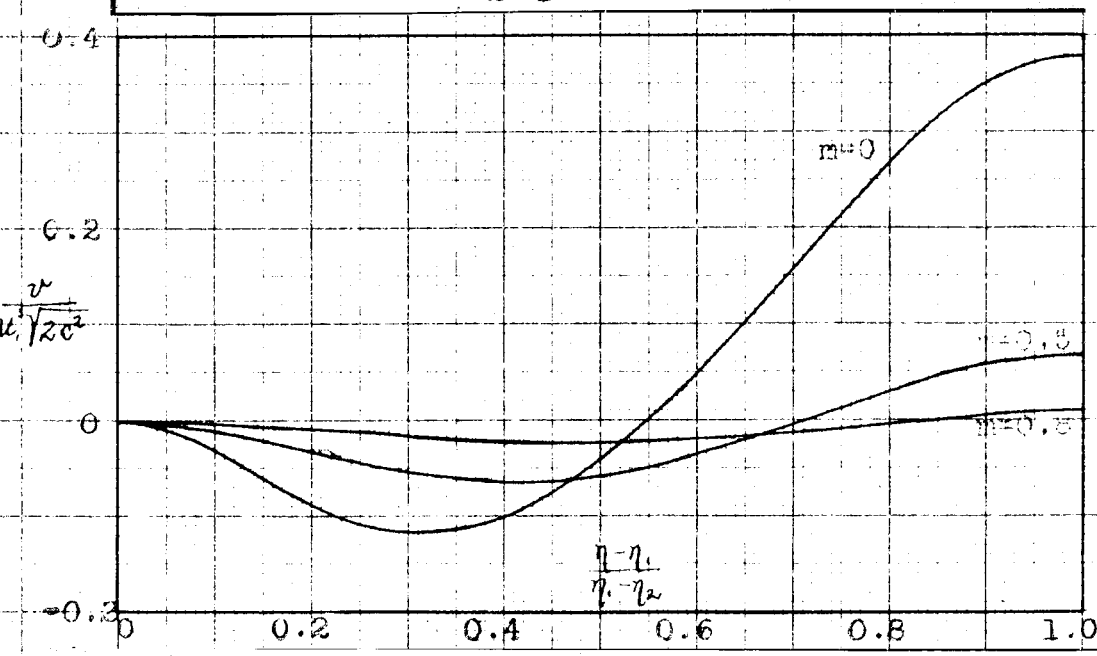

Figure 5. Distribution of $\frac{v}{u_1\sqrt[3]{2c^2}}$ for three values of $m = u_2/u_1$.

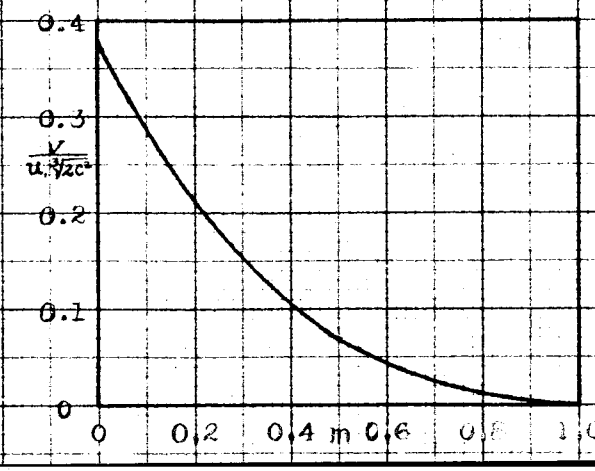

Figure 6. Suction Velocity at the low velocity boundary as a function of $m = u_2/u_1$.

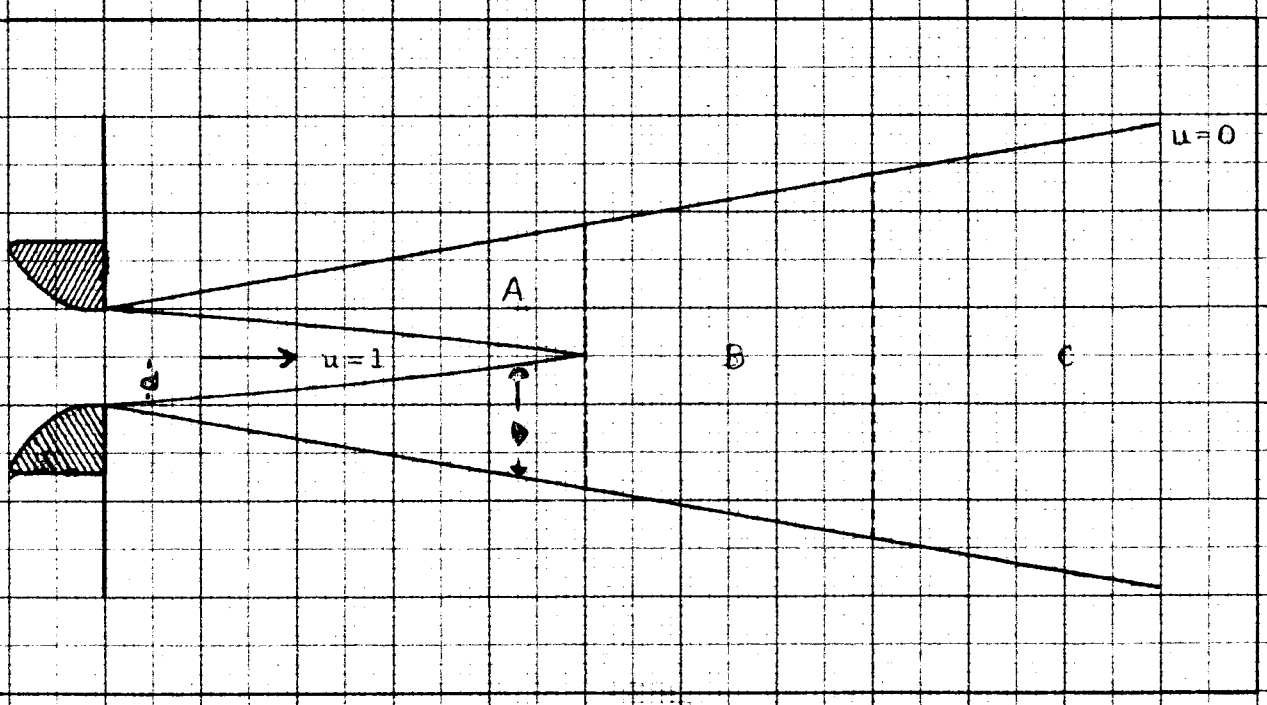

Figure 7. Schematic section of the flow from a circular nozzle.

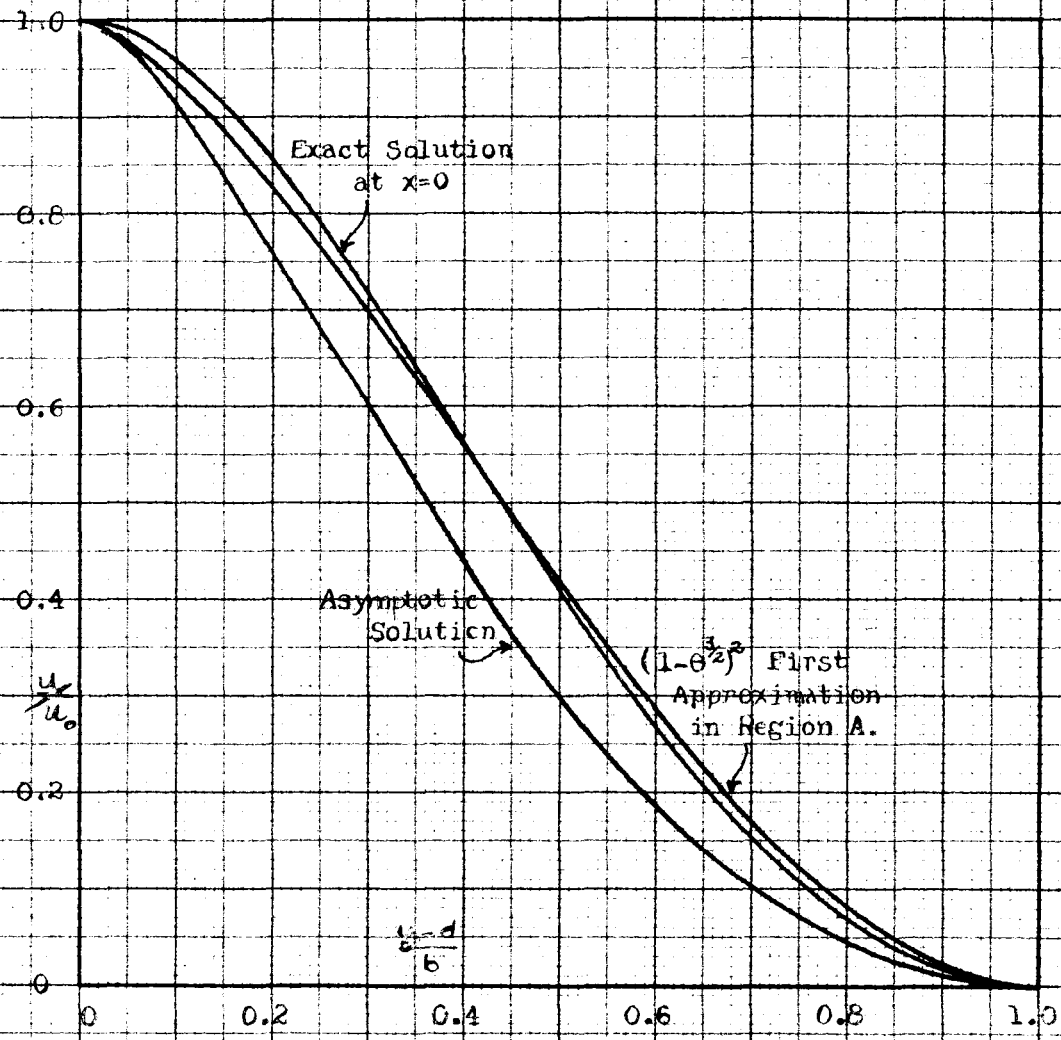

Figure 8. Comparison between solutions for x=0 and for x large. First approximation to all profiles in region A.

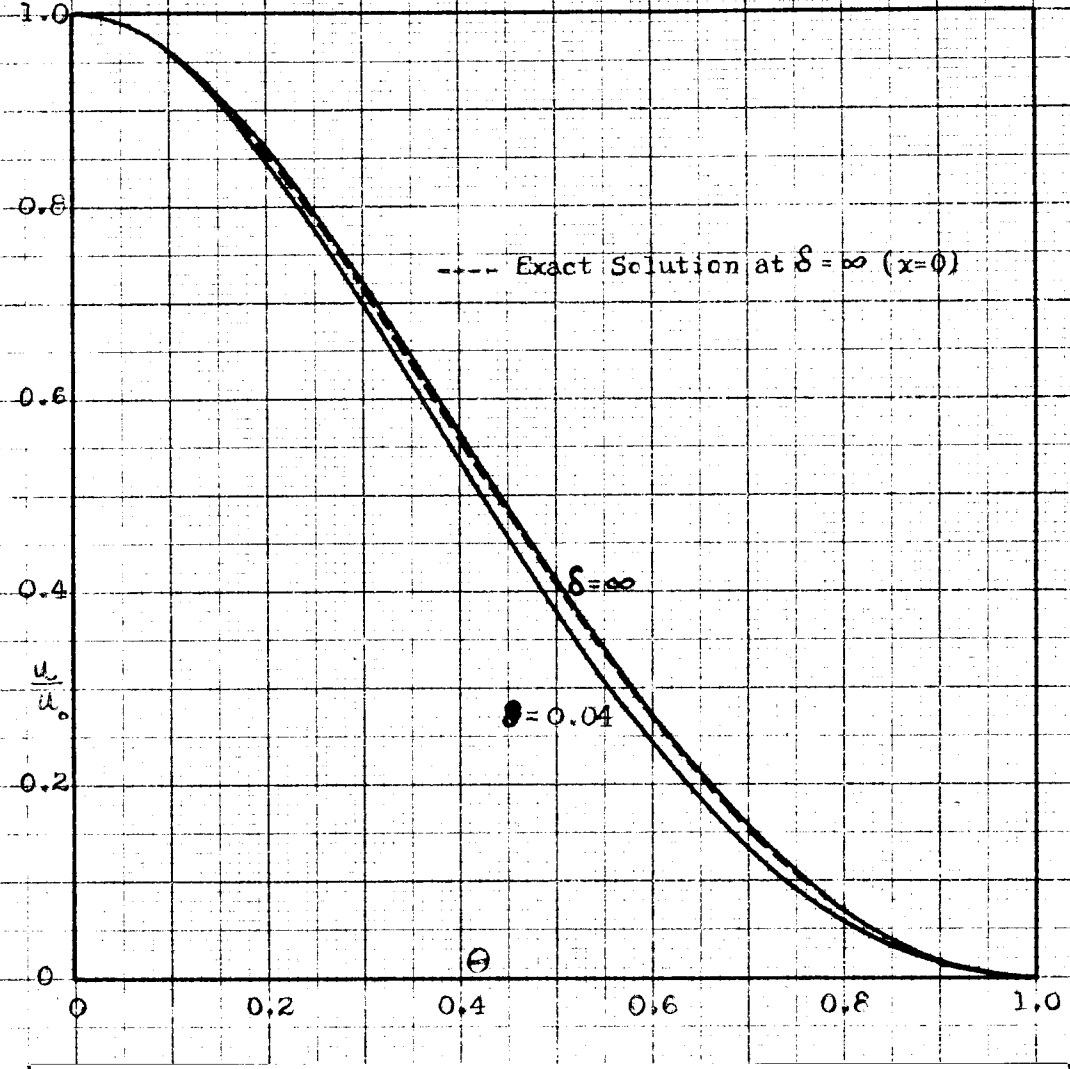

Figure 9. Second approximations to profiles in region A. Comparison between second approximation and exact solution for x=0.

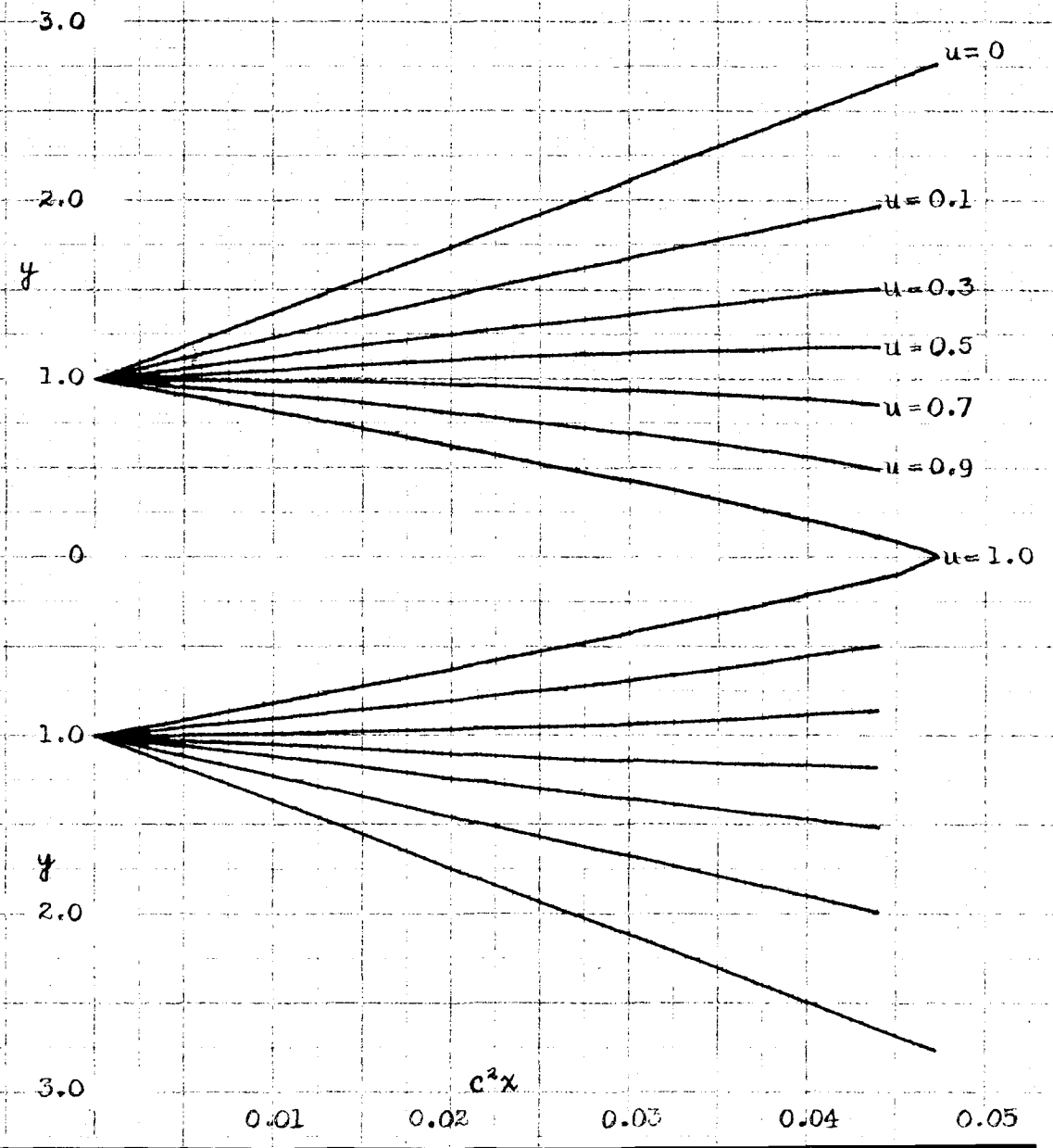

Figure 10. Second approximation to the velocity field in Region A.

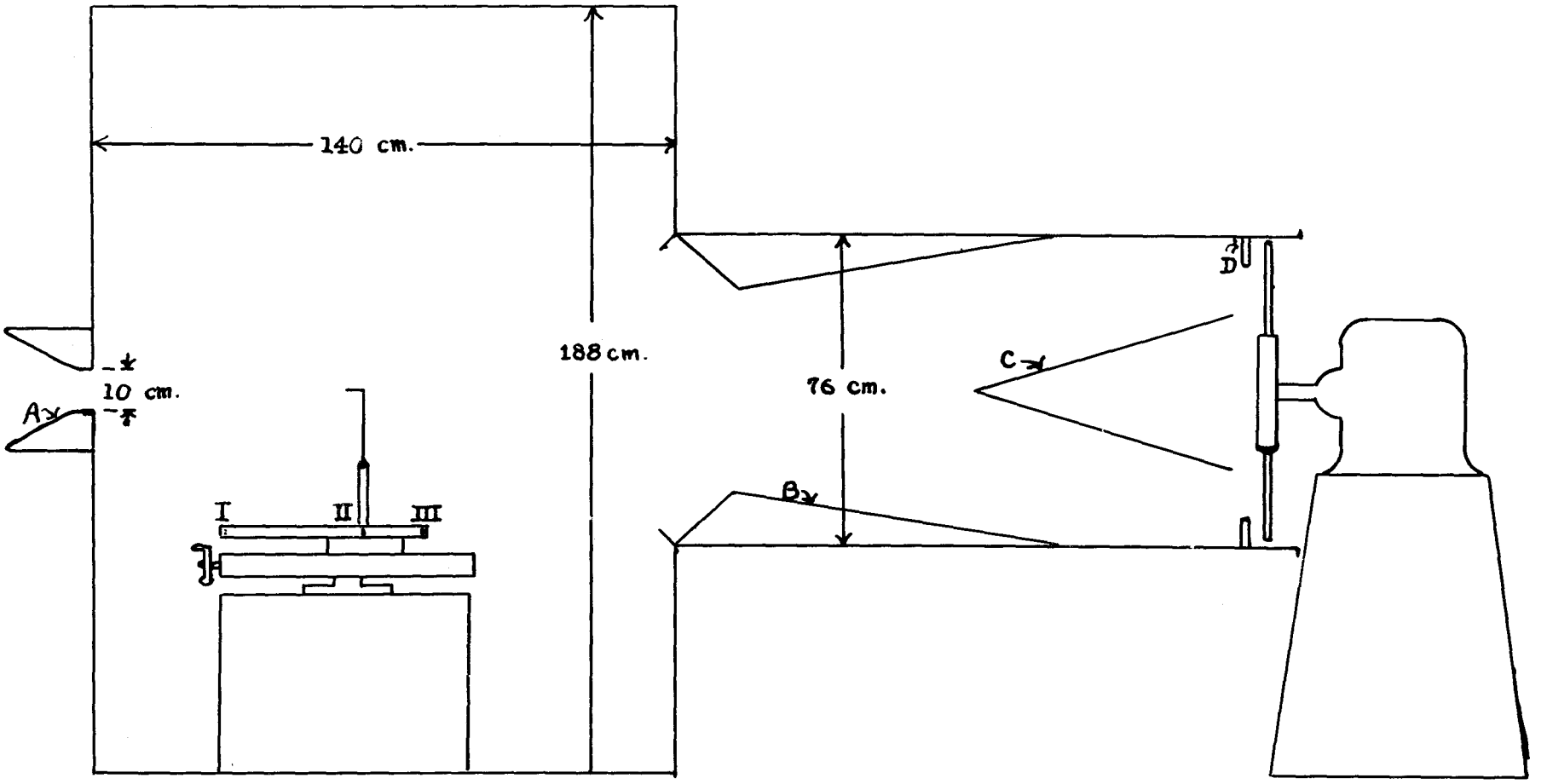

Figure 11. Longitudinal Section of Experimental Arrangement showing the measuring device in position.

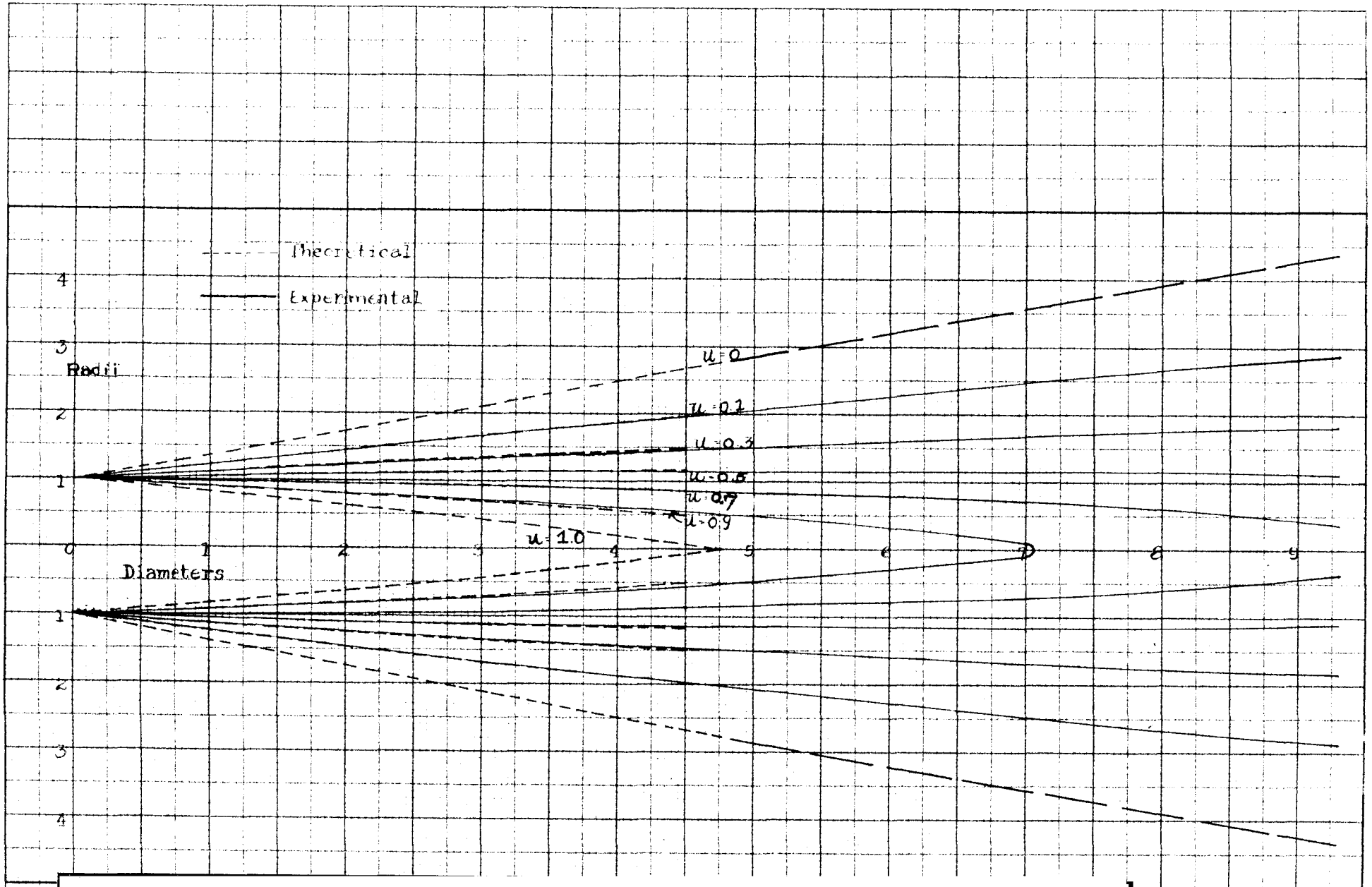

Figure 12. Experimentally determined velocity field of the jet and comparison with theory for $c^2 = 0.00496$. The boundaries of the jet at 9 diameters are calculated from Tollmien's solution for x large. Between 4.76 and 9 diameters the outer boundaries are interpolated.

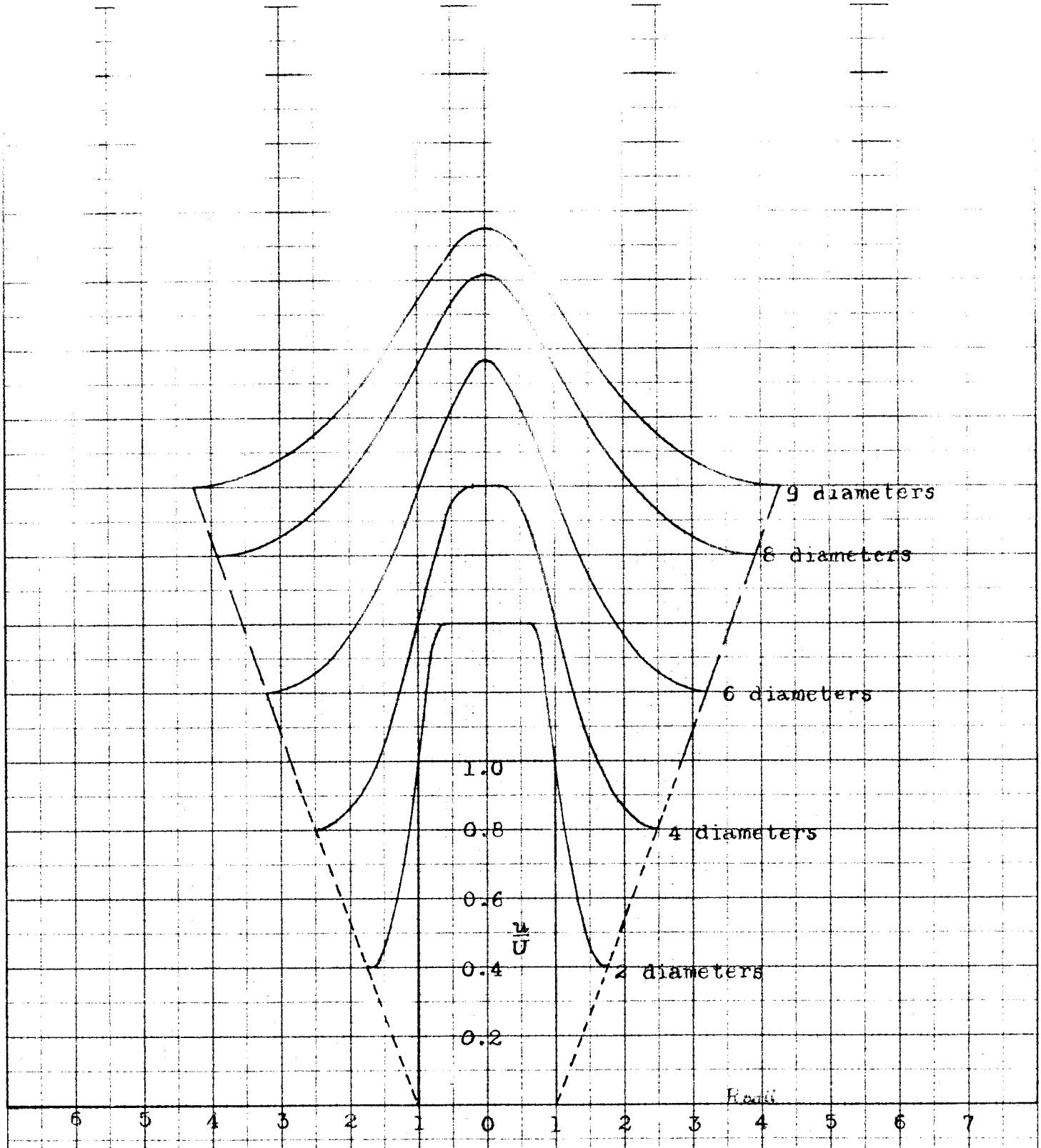

Figure 13. Experimental profiles at various distances from jet mouth. Outer boundaries are accentuated in the ratio 2:1. The ordinate is displaced 0.2D, where D is the number of diameters from the jet mouth, along the velocity axis.

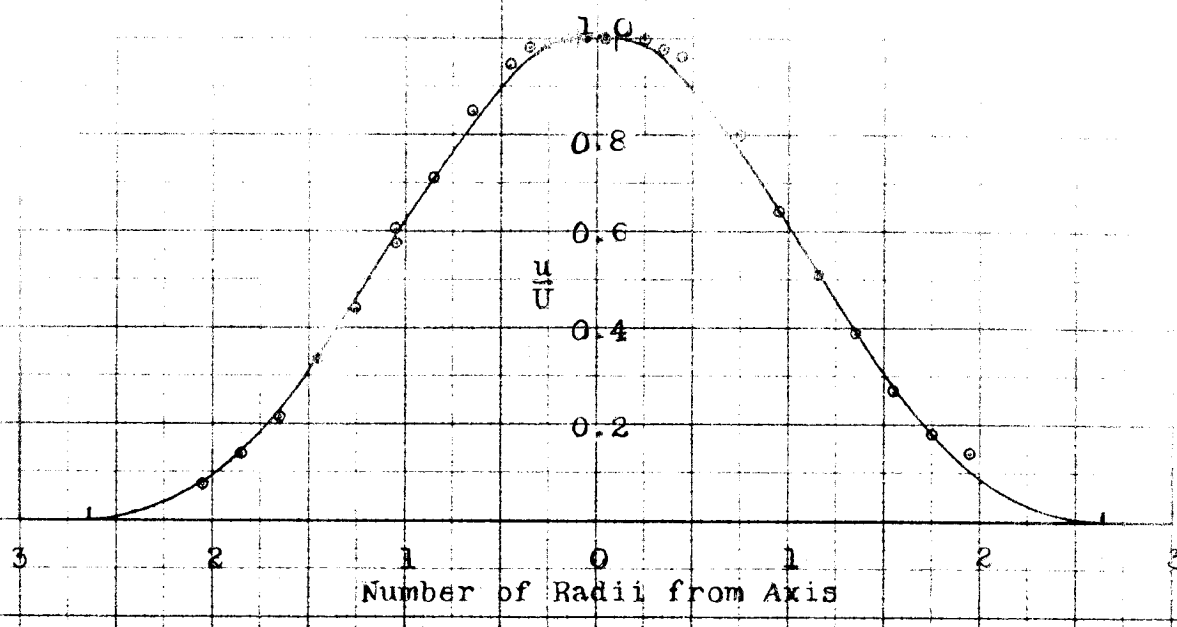

Figure 14. Comparison between theoretical profile and experimental points at x=4.5 diameters, which is the last point for which the theory is given. Vertical lines represent boundaries of the mixing region.

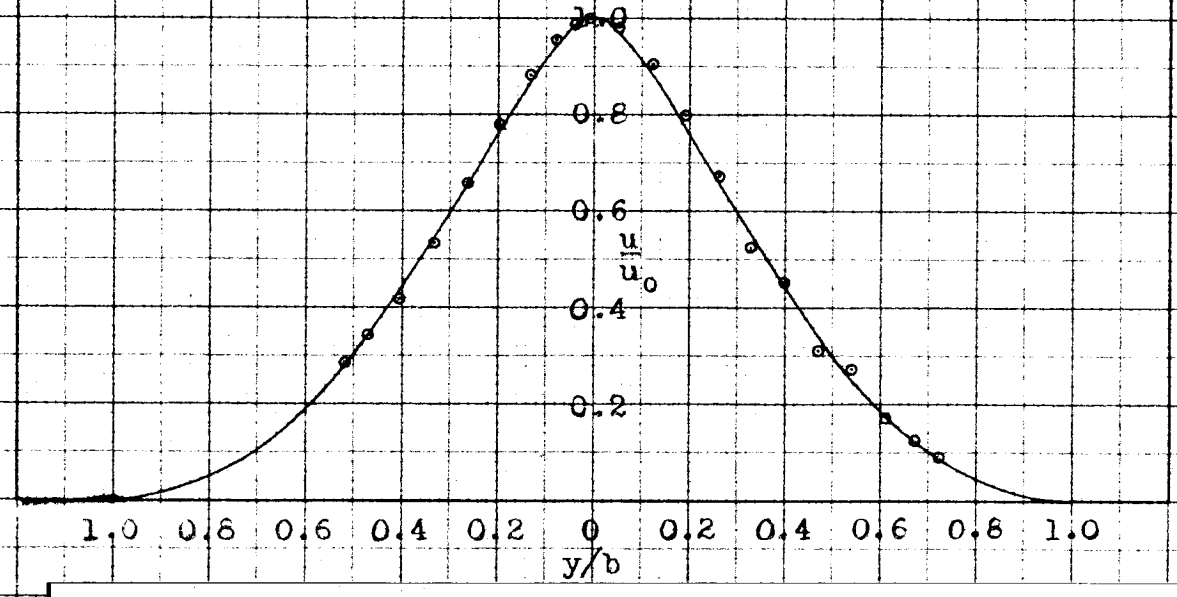

Figure 15. Comparison between Tollmien's theoretical profile for x large and the experimental points at x=9.3 diameters.

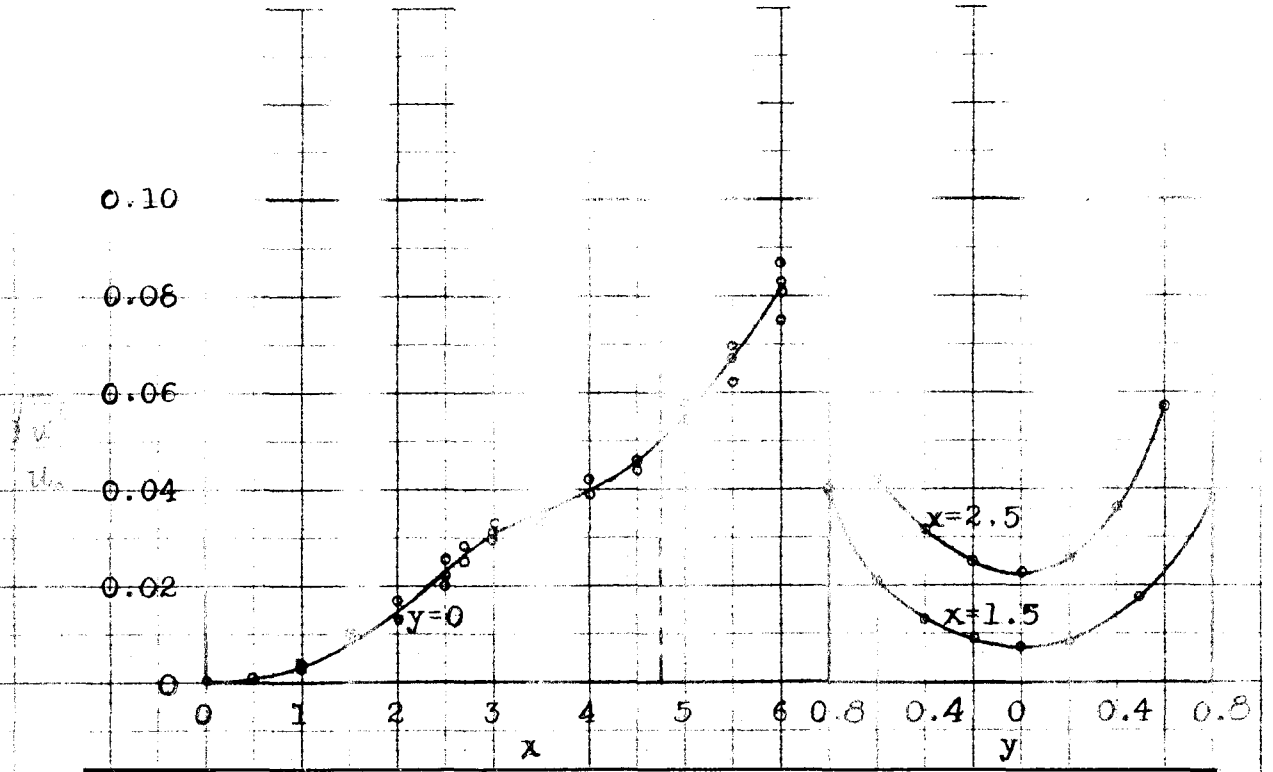

Figure 16. Root mean square velocity fluctuations along the axis of the jet. Broken line indicates the end of the core of potential flow. Lateral traverses across the potential core.

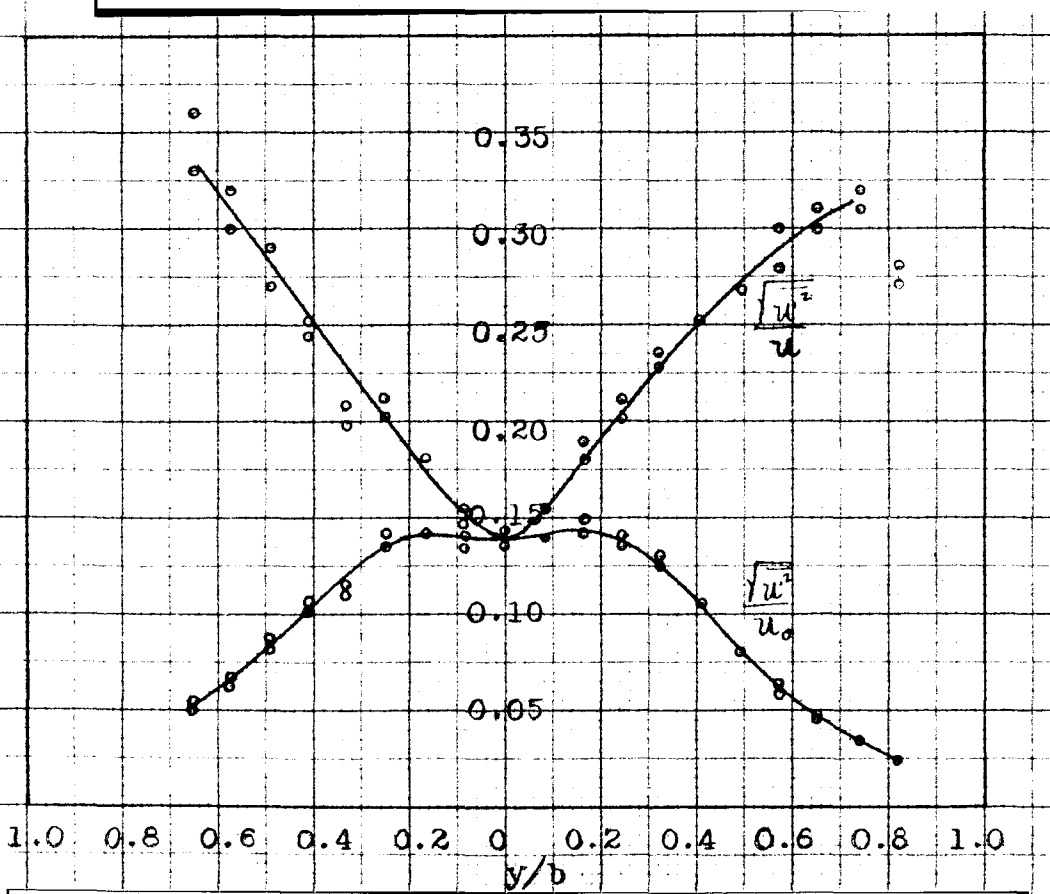

Figure 17. Root mean square velocity fluctuations across the mixing region at x = 9.0 diameters. $\sqrt{\overline{u^2}}/u_o$ is derived from the corresponding value for $\sqrt{\overline{u^2}}/u$.